

LETTERS

Global histone modification patterns predict risk of prostate cancer recurrence

David B. Seligson^{1*}, Steve Horvath^{2,3*}, Tao Shi^{2,3}, Hong Yu¹, Sheila Tze¹, Michael Grunstein⁴
& Siavash K. Kurdistani⁴

Aberrations in post-translational modifications of histones have been shown to occur in cancer cells but only at individual promoters¹; they have not been related to clinical outcome. Other than being targeted to promoters, modifications of histones, such as acetylation and methylation of lysine and arginine residues, also occur over large regions of chromatin including coding regions and non-promoter sequences, which are referred to as global histone modifications². Here we show that changes in global levels of individual histone modifications are also associated with cancer and that these changes are predictive of clinical outcome. Through immunohistochemical staining of primary prostatectomy tissue samples, we determined the percentage of cells that stained for the histone acetylation and dimethylation of five residues in histones H3 and H4. Grouping of samples with similar patterns of modifications identified two disease subtypes with distinct risks of tumour recurrence in patients with low-grade prostate cancer. These histone modification patterns were predictors of outcome independently of tumour stage, preoperative prostate-specific antigen levels, and capsule invasion. Thus, widespread changes in specific histone modifications indicate previously undescribed molecular heterogeneity in prostate cancer and might underlie the broad range of clinical behaviour in cancer patients.

Cancer of the prostate shows a heterogeneous clinical behaviour, from indolent to highly aggressive, and is the second leading cause of cancer deaths in men in the United States³. Present biomarkers including preoperative prostate-specific antigen (PSA) and biopsy Gleason score⁴ (a measure of tumour differentiation, scored from 2 to 10 with increasing degree of dedifferentiation) have not proved to be accurate predictors of clinical outcome⁵. The lack of prognostic markers is even more pressing in younger men with asymptomatic low-grade (Gleason score less than 7) tumours who are being increasingly identified by prevalent screening of PSA levels, but it is unclear how aggressively they should be treated^{6,7}. Improved prognostic markers are therefore needed.

Enzymes that modify histones show altered activity in cancer. For instance, missense mutations of p300 histone acetyltransferases and loss of heterozygosity at the p300 locus are associated with colorectal and breast cancers and with glioblastomas^{8–10}. The consequence of the altered activity of histone-modifying enzymes has so far been linked to inappropriate expression of few genes that might have a function in tumour biology. For instance, p300 is involved in androgen receptor transactivation, with a potentially important function in the progression of prostate cancer¹¹. However, in addition to being targeted to promoters, these enzymes also affect most

nucleosomes throughout the genome independently of apparent sequence-specific DNA-binding proteins^{2,12,13}. Furthermore, the histone-modifying enzymes possess a high degree of substrate specificity that differentiates between both the histone subtypes and the individual side chains within each histone^{14,15}. Thus, individual residues may be modified globally to various extents, reflecting the selective but widespread activity of the histone-modifying enzymes.

To determine the global levels of individual histone modifications in tissues obtained from patients, we combined immunohistochemistry, a method for detecting the presence of specific antigens in cells, with tissue microarrays (TMAs), for high-throughput analysis of many tissue samples¹⁶. We analysed the levels of acetylated (Ac) H3 Lys 9 (K9), K18 and H4 K12, and of dimethylated (diMe) H4 Arg 3 (R3) and H3 K4, using highly specific antibodies¹⁵ (Supplementary Fig. S1), on 183 primary prostate cancer tissues. The level of staining was assessed independently by two pathologists, who were blinded to all clinico-pathological variables. Here the global level of staining refers to the percentage of cells within each tissue sample that stained positively for a given antibody. For instance, Fig. 1a–d shows representative staining of four tissue samples, two each for H3 K18Ac (Fig. 1a, b) and H4 R3diMe (Fig. 1c, d) on tissue arrays. The cells with brown nuclei are considered positively stained. The unstained cells may still contain the modifications at certain genomic loci but their levels are below the detection limits, signifying that bulk histone modifications are considerably decreased in these cells. Immunostaining therefore reveals the presence or absence of global histone modifications in primary tissues.

To assess the differences in staining for the five antibodies, we plotted the frequencies (y axis) of tissue samples in which the indicated percentage cell staining (x axis) were observed for each modification (Fig. 1e). Acetylations of H3 K9 and K18 had very similar distributions, with more than 65% of samples showing 90–100% staining of the tumour cells. In contrast, only 16% of samples showed 90–100% staining for H4 K12; little or no acetylation was detected in about 24% of samples. Dimethylation of H3 K4 and H4 R3 showed broader distributions, with more than 60% of samples staining between 20% and 80% of cells. These data indicate that the levels of histone modifications differ considerably between individual tissues. We show below that these differences are important for defining groups of patients with distinct clinical outcomes.

We first wished to determine the relationship between levels of the five histone modifications and degree of differentiation (grade) for all samples. Of the five modifications, H3 K18Ac ($r = 0.28$, $P = 9.6 \times 10^{-5}$), H3 K4diMe ($r = 0.22$, $P = 3.4 \times 10^{-3}$),

¹Department of Pathology and Laboratory Medicine, David Geffen School of Medicine, University of California, Los Angeles, California 90095, USA. ²Department of Human Genetics, David Geffen School of Medicine, University of California, Los Angeles, California 90095, USA. ³Department of Biostatistics, School of Public Health, University of California, Los Angeles, California 90095, USA. ⁴Department of Biological Chemistry, David Geffen School of Medicine, University of California, Los Angeles, California 90095, USA.

*These authors contributed equally to this work.

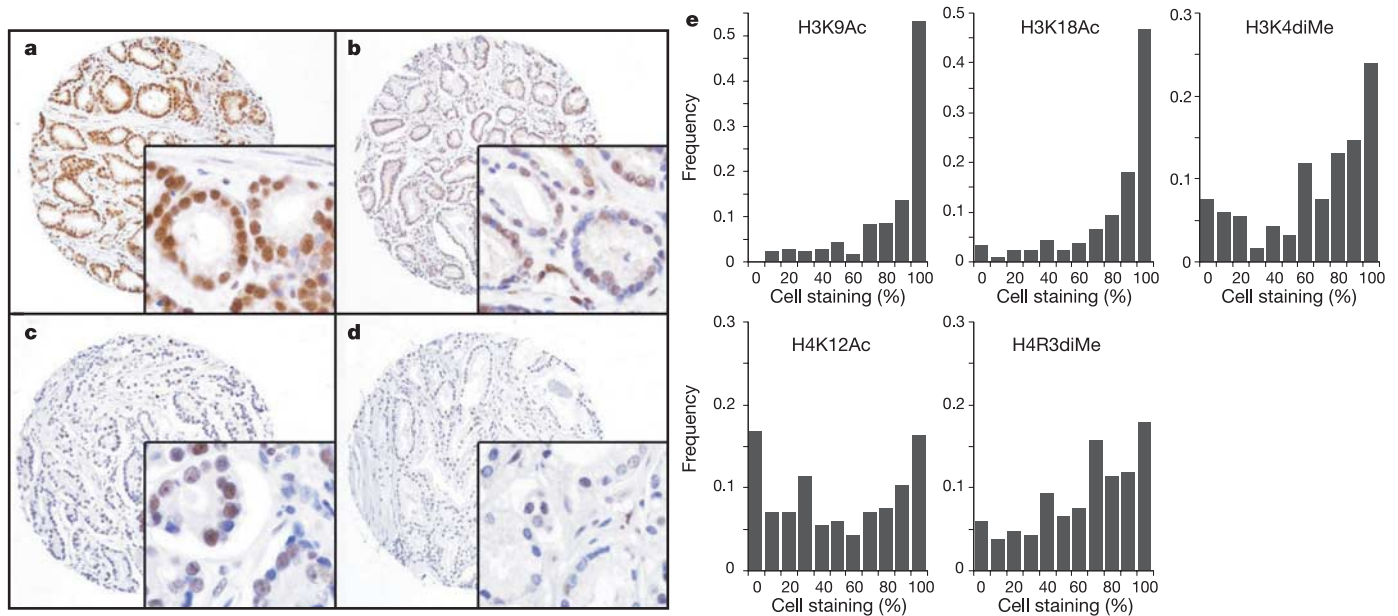


Figure 1 | Global levels of individual histone modifications are determined by immunohistochemistry. **a–d**, Characteristic nuclear staining of malignant prostate glandular cells by immunohistochemistry with antibodies against H3 K18 acetylation (**a**, **b**) or against H4 R3 dimethylation (**c**, **d**). Representative sections from group 1 patients with 95% (**a**) and 70%

(**c**) positive staining and of group 2 patients with 50% (**b**) and 25% (**d**) positive staining are shown (see Fig. 3). Original magnifications, $\times 10$; insets, $\times 40$. **e**, Distribution of staining for the five different antibodies across all 183 tissue samples. The y axis is the fraction of samples showing positive staining for the indicated percentage of cells (x axis).

H4 K12Ac ($r = 0.33$, $P = 4.8 \times 10^{-6}$) and H4 R3diMe ($r = 0.23$, $P = 2.0 \times 10^{-3}$) are positively correlated with increasing grade but H3 K9Ac ($r = 0.11$, $P = 1.4 \times 10^{-1}$) shows no significant correlation. Despite the positive correlations with grades, none of the modifications is associated individually with the risk of tumour recurrence (Supplementary Table S1). The significance of these correlations is unclear, but the higher levels of staining might be related to the increased proliferative capacity of dedifferentiated tumours, which might be associated with increased gene activity. In this regard, H3 K18Ac and H4 R3diMe are two histone modifications associated with gene activity^{17,18}.

The relationships described above are between individual modifications and grade for all patient samples. To determine whether unique patterns of histone modifications, involving combinations of the five sites, were shared between subsets of tissue samples, we

applied the random forest (RF) clustering algorithm to the data^{19–21}. RF clustering is an unsupervised classification method that, by generating an ensemble of individual tree predictors, leads to a measure of natural dissimilarity between the observations. The result of the RF clustering of all 183 samples is shown in Fig. 2a as a multidimensional scaling (MDS) plot. In MDS plots, the orientation and unit of axes are arbitrary but increasing distances between data points reflect increasing degree of dissimilarity. Each patient sample is labelled according to its Gleason score. As delineated by the blue line in Fig. 2a, two groups of patients were identified by inspection and are colour-coded as red ($n = 70$) and black ($n = 113$). In Kaplan–Meier²² survival analysis, we did not detect a statistically significant difference in the risk of tumour recurrence between these two groups (Fig. 2b).

However, further stratification of patients into high-grade (Gleason

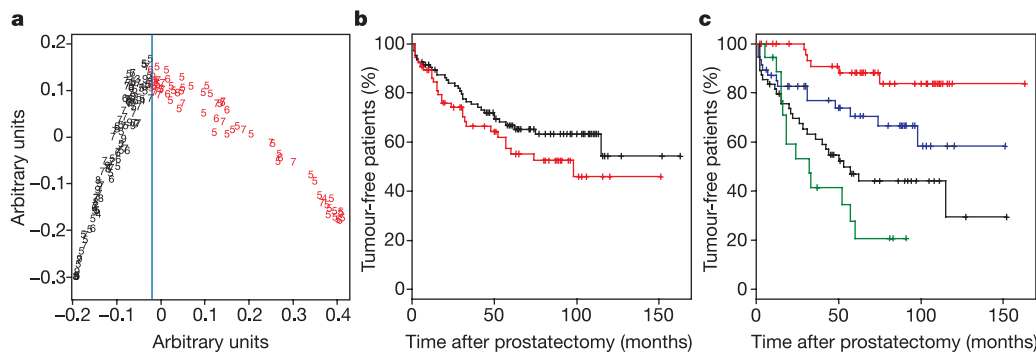


Figure 2 | Grouping of patients with similar histone modification patterns. **a**, An MDS plot is used to visualize the degree of dissimilarity (distance along the axes with arbitrary units) between all patients (with low-grade and high-grade tumours) as generated by the RF algorithm on the basis of the histone modification patterns. Patients are indicated by their Gleason score. Two groups are identified by inspection (blue line dividing

the sample into group 1 (black) and group 2 (red)). **b**, Kaplan–Meier recurrence-free plots of the two groups (black, group 1; red, group 2) identified among all patients. Log-rank $P = 0.178$. **c**, Kaplan–Meier recurrence-free survival plots based on modification pattern grouping (as in **a**) and grade stratification (blue and red lines, patients with low-grade tumours; green and black lines, patients with high-grade tumours).

score 7–10) and low-grade (Gleason score 2–6) patients revealed two subgroups within each category of patients with a considerable difference in their risk of tumour recurrence (Fig. 2c; compare red with blue lines and green with black lines). These results indicate that the differences in histone modification patterns might be a better predictor of clinical outcome when patients are first stratified broadly on the basis of grade. We therefore first stratified patients into those with a Gleason score of 7 or more ($n = 79$) and those with a Gleason score of less than 7 ($n = 104$; Supplementary Table S2), and then applied the RF clustering algorithm. In the patients with high-grade tumours, distinct groups based on histone modifications were not clearly evident (data not shown). However, among the patients with low-grade tumours we found two groups of patients by inspection (Fig. 3a). The median levels and distribution of staining for the various modifications in the two groups are shown in the box plots²³ of Fig. 3b. As expected from the clustering, the two groups show different modification patterns. For instance, the median per cent cell staining for H3 K9Ac in group 1 is 90%, whereas that in group 2 is 16%. Within each group of patients, different histone modifications showed differential levels of staining. For instance, within group 1, the median percentage cell staining for H3 K9Ac was 100%, whereas that for H4 K12Ac was 68%. Similarly, within group 2, the median percentage cell staining for H3 K18Ac was 52%, whereas that for H4 K12Ac was 5%. Taken together, these observations indicate that groups of patients can be identified on the basis of similar combinations of global histone modifications.

To ascertain whether the identified groups are clinically significant, we determined the risk of tumour recurrence in each group after removal of the primary tumour (Fig. 4a). Remarkably, the patients in group 1 had a lower risk of 10-year tumour recurrence (17%) when compared with those in group 2 (42%) ($P = 0.0076$). Grade does not substitute for the histone modifications because there was no significant difference in the distribution of patients based on the Gleason score between the two groups (Fisher's exact test, $P > 0.2$; Fig. 4a). We also asked whether the modification patterns added prognostic information beyond other known prognostic factors. We found that the histone modification patterns predicted tumour recurrence independently of tumour stage, preoperative PSA, and capsule invasion (Table 1). Specific patterns of global histone modifications therefore represent independent molecular markers associated with distinct clinical outcomes.

Although all five modification sites contributed to the grouping of patients above, the groups identified can also be estimated from less information. For instance, group 1 individuals with a lower risk of tumour recurrence can be identified as those patients who are above

Table 1 | Multivariate proportional hazard analysis

Variable	Hazard ratio	95% CI	P
Tumour stage	7.54	(1.86–30.47)	0.0046
Preoperative serum PSA (ng ml^{-1})	1.02	(0.98–1.07)	0.3100
Capsule invasion	3.41	(1.40–8.30)	0.0070
Histone modification patterns	3.86	(1.18–12.62)	0.0250

the 60 percentile staining for H3 K4diMe or above 35 percentile staining for H3 K18Ac and above 35 percentile staining for H3 K4diMe; those patients that do not satisfy this rule belong to group 2 (Supplementary Fig. S2). When this rule is used to predict recurrence risk, it results in only two misclassified patients (log-rank $P = 0.028$; hazard ratio = 2.8; 95% confidence interval (CI) 1.12–7.02). Thus, although additional information leads to more significant groupings, simpler rules involving a limited number of modifications can be constructed that might prove to be more practicable in clinical settings.

To validate the prognostic power of histone modifications, an additional independent set of 39 patient samples with low-grade prostate cancer (obtained from the University of Michigan Medical School) was analysed according to the above simple rule involving H3 K18Ac and K4diMe staining (Supplementary Table S3). As shown in Fig. 4b, the staining distinguishes between two groups of patients with distinct risks of tumour recurrence: 4% in group A versus 31% in group B (log-rank $P = 0.016$; hazard ratio = 9.2; 95% CI 1.02–82.2). There is no significant difference in the distribution of patients based on the Gleason score between the two groups (Fisher's exact test, $P > 0.2$; Fig. 4b). The prognostic classification on the validation set therefore confirms the predictive power of histone modifications as markers of prognosis.

We have provided evidence that changes in bulk histone modifications of cancer cells are predictive of clinical outcome. The mechanistic basis of such changes are currently unclear but may be related to the altered expression and/or global activities of various histone-modifying enzymes. The variability in the levels of any one modification was not sufficient for predicting outcome. However, in combination, these changes proved to be indicative of the risk of tumour recurrence in patients with low-grade prostate cancer. Considering the substantial number of modifications on histones, it is possible that information on global patterns of other modification sites will help with the further classification of all patients, including those in the high-grade category. The utility of immunohistochemistry, combined with the availability of an extensive set of

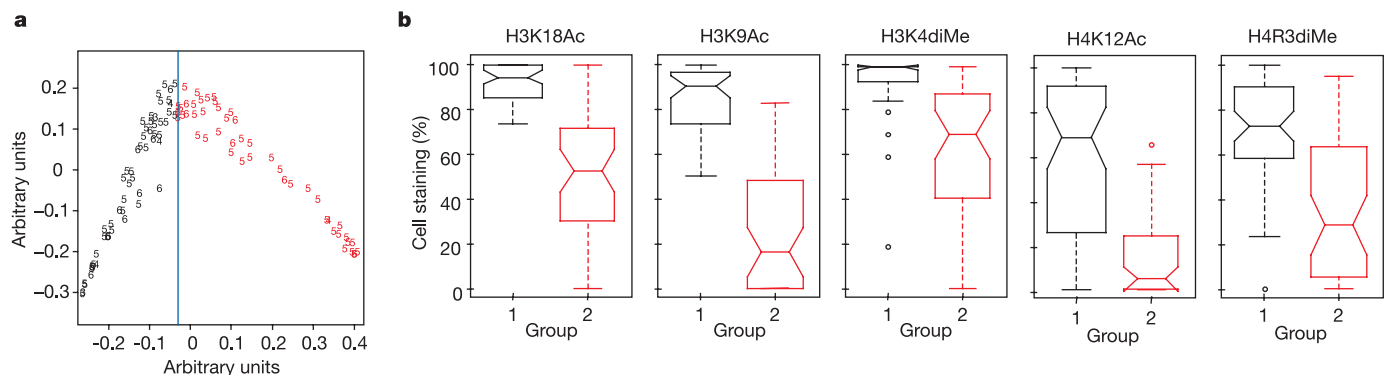


Figure 3 | Grouping of patients with low-grade tumours with similar histone modification patterns. **a**, An MDS plot showing the degree of dissimilarity between patients with low-grade tumours as generated by the RF algorithm. Patients are indicated by their Gleason score. Two groups are identified by inspection (blue line dividing the sample into group 1 (black)

and group 2 (red)). **b**, The distributions of staining for the five histone modifications in group 1 (black) and group 2 (red) patients are shown as box plots. The line in the centre of each box represents the median value of the distribution, and the upper and lower ends of the box are the upper (25th) and lower (75th) quartiles, respectively. The whiskers show the ranges.

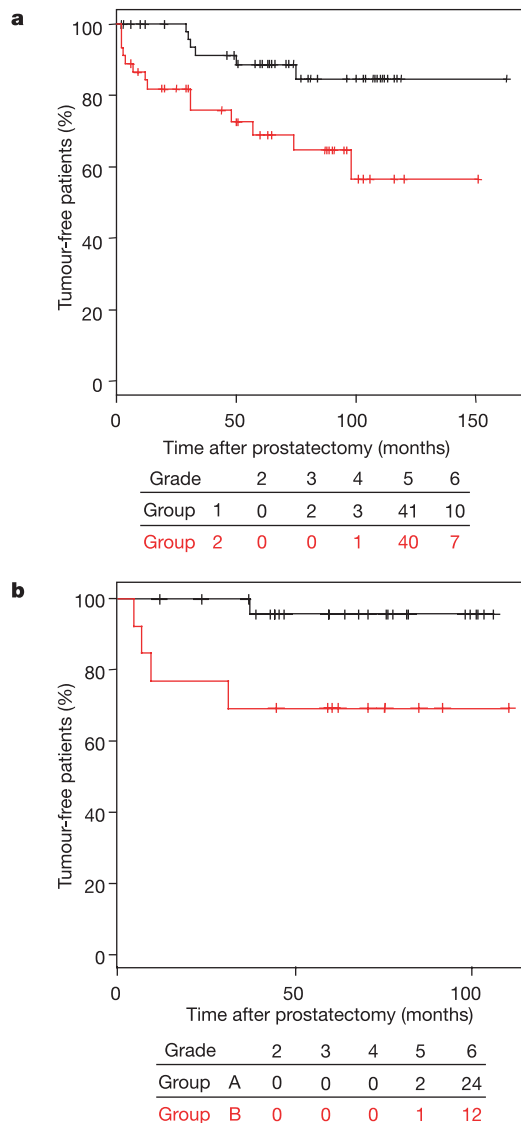


Figure 4 | Histone modification patterns predict tumour recurrence. **a**, Kaplan–Meier recurrence-free plots of the two groups (black, group 1; red, group 2) identified among the patients with low-grade tumours ($n = 104$; UCLA) based on the histone modification patterns. Log-rank $P = 0.0076$. Tabulated below is the distribution of the patients in each group according to their grade (Gleason score). **b**, Kaplan–Meier recurrence-free plots of the two groups (black, group A; red, group B) identified among the patients with low-grade tumours of the validation data set ($n = 39$; University of Michigan). The two groups are identified on the basis of the ‘simple rule’ involving only H3 K18Ac and H3 K4diMe modifications. Log-rank $P = 0.016$. The distribution of the patients in each group according to their grade is tabulated below.

antibodies to probe histone modifications, should facilitate the application of our approach to other tumours. It is conceivable that patterns of histone modifications including those reported here might also serve as prognostic or even diagnostic markers in other types of cancer.

Note added in proof: While this paper was being peer-reviewed, it was reported that acetylation of H4 K16 and trimethylation of H4 K20 are reduced at repetitive DNA sequences in multiple cancer types²⁴.

METHODS

Prostate TMA. A prostate TMA was constructed with formalin-fixed, paraffin-embedded prostate tissue samples as described previously¹⁶. At least three replicate tumour samples were taken from donor tissue blocks in a highly

representative fashion. Twenty patients treated with neoadjuvant hormones were excluded from the study. In total, 183 cases were informative for all five histone markers; 171 of those were supported by complete recurrence data. A retrospective analysis for outcome assessment was based on detailed anonymized clinico-pathological information linked to the TMA specimens. Recurrence, defined as a postoperative serum PSA of 0.2 ng ml^{-1} or more, was seen in 61 (34%) of all study patients and in 20 (19%) of patients with low-grade tumours. The median total follow-up, defined as the time to recurrence or to last contact in non-recurring patients, was 60.0 months (range 2–163) for patients with low-grade tumours. The median follow-up time within the recurring and non-recurring patient groups was 30.5 months (2.0–98.0) and 65.5 months (range 2.0–163.0), respectively, in patients with low-grade tumours. The validation data set was generated from prostate TMAs that were purchased from the University of Michigan Medical School (Supplementary Table S3).

Immunohistochemistry. The antibodies were first tested and optimized on whole-tissue sections and test arrays. Once an appropriate dilution had been determined, a set of three slides containing all patient samples were stained for each antibody, using standard two-step indirect immunohistochemistry. Tissue array sections were cut with of a sectioning aid (Instrumedics) immediately before being stained. After deparaffinization in xylenes, the sections were rehydrated in graded alcohols. Endogenous peroxidase was quenched with 3% hydrogen peroxide in methanol at room temperature (25°C). The sections were placed in a 95°C solution of 0.01 M sodium citrate buffer pH 6.0 for antigen retrieval. Normal goat serum (5%) was next applied for 30 min to block non-specific protein-binding sites. Primary rabbit anti-histone polyclonal antibodies were applied for 30 min at room temperature at the following dilutions: H3 K18Ac at 1:200, H3 K9Ac at 1:800, H4 K12Ac at 1:100, H3 K4diMe (Abcam) at 1:800, and H4 R3diMe (Upstate) at 1:25. Detection was accomplished with the Dako Envision System, followed by chromogen detection with diaminobenzidine (DAB). The sections were counterstained with Harris’s haematoxylin, followed by dehydration and mounting. Negative controls were identical array sections stained in the absence of the primary antibody. Semiquantitative assessment of antibody staining on the TMAs was performed by H.Y. and D.B.S., who were blinded to all clinico-pathological variables. The frequency of nuclear positive target cells (range 0–100%) in prostatic glandular epithelium was scored for each TMA spot.

Unsupervised clustering algorithm. To facilitate unsupervised learning, an intrinsic dissimilarity measure between the patients was constructed with an RF analysis of the histone markers. A technical description of the RF clustering algorithm is given in Supplementary Methods and <http://www.genetics.ucla.edu/labs/horvath/RFclustering/RFclustering.htm>. The RF clustering algorithm was shown recently to be particularly suitable for TMA data for the following reasons²¹. First, the clustering results do not change when one or more covariates are monotonically transformed, because the dissimilarity depends only on the feature ranks, obviating the need for symmetrizing skewed covariate distributions. Second, the RF dissimilarity weights the contributions of each covariate on the dissimilarity in a natural way: the more related the covariate is to other covariates the more it will affect the definition of the RF dissimilarity. Third, the RF dissimilarity does not require the user to specify threshold values for dichotomizing tumour expressions. External threshold values for dichotomizing expressions in unsupervised analyses may reduce the information content or even bias the results. We also compared the RF clustering approach with the standard euclidean distance-based approach. Although there is good overlap between the two algorithms, we find that the RF clustering method works better for these data (Supplementary Methods). To reveal the clustering, we used classical MDS, which takes as input the RF dissimilarity between the samples and returns a set of points in a two-dimensional space such that the distances between the points are approximately equivalent to the original distances.

Statistical analysis. To test whether variables differed across groups, we used the Kruskal–Wallis test. To visualize the survival distributions, we used Kaplan–Meier plots. The Cox proportional hazards model was used to test the statistical independence and significance of predictors. The proportional hazard assumption was tested by using scaled Schoenfeld residuals. Log-rank tests were used to test the difference between survival distributions. All P values were two-sided, and $P < 0.05$ was considered significant. All statistical analyses were performed with the freely available software R (<http://www.R-project.org/>). R code that implements RF clustering is available from the authors on request.

Further details. A more detailed description of the methods used is given in the Supplementary Methods.

Received 21 February; accepted 25 April 2005.

- Jacobson, S. & Pillus, L. Modifying chromatin and concepts of cancer. *Curr. Opin. Genet. Dev.* 9, 175–184 (1999).

2. Vogelauer, M., Wu, J., Suka, N. & Grunstein, M. Global histone acetylation and deacetylation in yeast. *Nature* **408**, 495–498 (2000).
3. Jemal, A. *et al.* Cancer statistics, 2003. *CA Cancer J. Clinicians* **53**, 5–26 (2003).
4. Gleason, D. F. Classification of prostatic carcinomas. *Cancer Chemother. Rep.* **50**, 125–128 (1966).
5. Bunting, P. S. Screening for prostate cancer with prostate-specific antigen: beware the biases. *Clin. Chim. Acta* **315**, 71–97 (2002).
6. Han, M., Partin, A. W., Piantadosi, S., Epstein, J. I. & Walsh, P. C. Era specific biochemical recurrence-free survival following radical prostatectomy for clinically localized prostate cancer. *J. Urol.* **166**, 416–419 (2001).
7. Farkas, A., Schneider, D., Perrotti, M., Cummings, K. B. & Ward, W. S. National trends in the epidemiology of prostate cancer, 1973 to 1994: evidence for the effectiveness of prostate-specific antigen screening. *Urology* **52**, 444–448 (1998).
8. Giles, R. H., Peters, D. J. & Breuning, M. H. Conjunction dysfunction: CBP/p300 in human disease. *Trends Genet.* **14**, 178–183 (1998).
9. Gayther, S. A. *et al.* Mutations truncating the EP300 acetylase in human cancers. *Nature Genet.* **24**, 300–303 (2000).
10. Muraoka, M. *et al.* p300 gene alterations in colorectal and gastric carcinomas. *Oncogene* **12**, 1565–1569 (1996).
11. Debes, J. D. *et al.* p300 in prostate cancer proliferation and progression. *Cancer Res.* **63**, 7638–7640 (2003).
12. Reid, J. L., Iyer, V. R., Brown, P. O. & Struhl, K. Coordinate regulation of yeast ribosomal protein genes is associated with targeted recruitment of Esa1 histone acetylase. *Mol. Cell* **6**, 1297–1307 (2000).
13. Krebs, J. E., Fry, C. J., Samuels, M. L. & Peterson, C. L. Global role for chromatin remodeling enzymes in mitotic gene expression. *Cell* **102**, 587–598 (2000).
14. Peterson, C. L. & Laniel, M. A. Histones and histone modifications. *Curr. Biol.* **14**, R546–R551 (2004).
15. Suka, N., Suka, Y., Carmen, A. A., Wu, J. & Grunstein, M. Highly specific antibodies determine histone acetylation site usage in yeast heterochromatin and euchromatin. *Mol. Cell* **8**, 473–479 (2001).
16. Kononen, J. *et al.* Tissue microarrays for high-throughput molecular profiling of tumour specimens. *Nature Med.* **4**, 844–847 (1998).
17. Kurdistani, S. K., Tavazoie, S. & Grunstein, M. Mapping global histone acetylation patterns to gene expression. *Cell* **117**, 721–733 (2004).
18. Rezaei-Zadeh, N. *et al.* Targeted recruitment of a histone H4-specific methyltransferase by the transcription factor YY1. *Genes Dev.* **17**, 1019–1029 (2003).
19. Breiman, L. *Classification and Regression Trees* (Wadsworth International, Belmont, California, 1984).
20. Breiman, L. Random forests. *Mach. Learn.* **45**, 5–32 (2001).
21. Shi, T., Seligson, D., Beldegrun, A. S., Palotie, A. & Horvath, S. Tumor classification by tissue microarray profiling: random forest clustering applied to renal cell carcinoma. *Mod. Pathol.* **18**, 547–557 (2005).
22. Kaplan, E. & Meier, P. Nonparametric estimation from incomplete observations. *J. Am. Stat. Assoc.* **53**, 457–481 (1958).
23. Cleveland, W. S. *Visualizing Data* (Hobart Press, Murray Hill, New Jersey, 1993).
24. Fraga, M. F. *et al.* Loss of acetylation at Lys16 and trimethylation at Lys20 of histone H4 is a common hallmark of human cancer. *Nature Genet.* **37**, 391–400 (2005).

Supplementary Information is linked to the online version of the paper at www.nature.com/nature.

Acknowledgements We thank M. Vogelauer for suggestions on the manuscript, and V. Minin for help with the statistical analyses. T.S. was a doctoral trainee supported by the UCLA Integrative Graduate Education and Research Traineeship (IGERT) Bioinformatics Program funded by the NSF Division of Graduate Education (DGE). This work was funded partly by a National Cancer Institute (NCI) grant through the Jonsson Comprehensive Cancer Center to D.B.S. and a Howard Hughes Medical Institute Fellowship and a UCLA Specialized Program Of Research Excellence (SPORE) in Prostate Cancer Career Development grant to S.K.K.

Author Information Reprints and permissions information is available at npg.nature.com/reprintsandpermissions. The authors declare no competing financial interests. Correspondence and requests for materials should be addressed to S.K.K. (skurdistani@mednet.ucla.edu).